Published in The Journal of Imaging Science and Technology 41, issue 5, 488-496, 1997
which should be used for any reference to this work

From Holography To Micro-Optics

H. P. Herzig
Institute of Microtechnology, University of Neuchâtel, Switzerland

P. Ehbets
National Optics Institute, Sainte-Foy, Québec, Canada

Holography can store wavefields in light-sensitive material. Due to its flexibility and the potential of multiplexing several functions into one element, holography has also been proposed as a recording technique for micro-optical elements. This paper discusses the recording of holograms that perform the basic functionalities (deflection, focusing, and fan-out) needed in micro-optical systems. Emphasis is given to the optimum recording of fan-out elements and high-density multifacet holograms. Successful recording schemes are presented, which are easy to align and therefore are interesting for the fabrication of systems. The potential of holography is demonstrated by recording 10,000 lenslets on 1 cm^2 in a compact optical system. In addition, several highly efficient fan-out elements have been recorded as volume and surface-relief holograms.

Introduction

Holography is a successful technique to store wavefields in light-sensitive material. This technique has also been proposed to fabricate planar optical elements, such as gratings, lenses, and multiple-beam splitters.

During the last few years, diffractive optical elements (DOEs), which are realized as surface-relief grating structures from a computer-generated design by microfabrication technologies (electron-beam writing, photolithography, and etching), have gained significant importance.[1,2] In contrast to holographically recorded elements, their surface-relief structure can be realized in rigid substrate materials and has the potential to be mass fabricated at low cost by batch processing or replication technologies. Without lowering the potential of modern DOEs, we would like to emphasize in this paper some advantages of holographic recording, which show that the method is still of interest for the fabrication of miniaturized optical microsystems.

An example of a compact micro-optical system is shown in Fig. 1. A light source has to be connected to many detectors. The problems to solve are as follows:

1. fabrication of off-axis elements requiring structures with >1000 lines/mm,
2. short distance requiring high numerical aperture and large fan-out angle,
3. large (N × N) arrays requiring high accuracy and no distortion, and
4. high diffraction efficiency and low stray light.

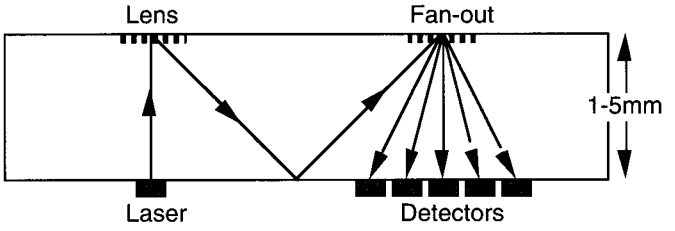

Figure 1. Planar micro-optical system connecting a source to many detectors.

Holography is ideal to fabricate off-axis elements with small feature sizes. The absolute position accuracy of the recorded grating structures is considerably higher than that achievable with electron-beam writing which suffers from stitching errors.[3]

For asymmetric deflection (Fig. 1), surface-relief gratings require a well-controlled blazed profile in order to attain a high diffraction efficiency. Such fine grating profiles still impose problems for the fabrication.[4,5] In holographic recording, high diffraction efficiencies over 90% can be achieved by recording a volume hologram and using readout at the Bragg angle. However, in order to achieve this performance with complex holograms (for example, the fan-out element shown in Fig. 1), special care has to be taken at recording. The fan-out operation can be realized either by a multiplexed grating or by a multifacet hologram. The multiplexed fan-out grating offers a higher interconnection density, whereas the multifacet HOE allows more flexibility for arbitrary focusing and interconnections. In this paper, we discuss both approaches and present optimum recording schemes which enable high diffraction efficiency and good reconstruction fidelity and which are also applicable for generating large arrays of beams.

A serious problem is the aberrations (distortion) and fabrication tolerances of optical elements. These errors can

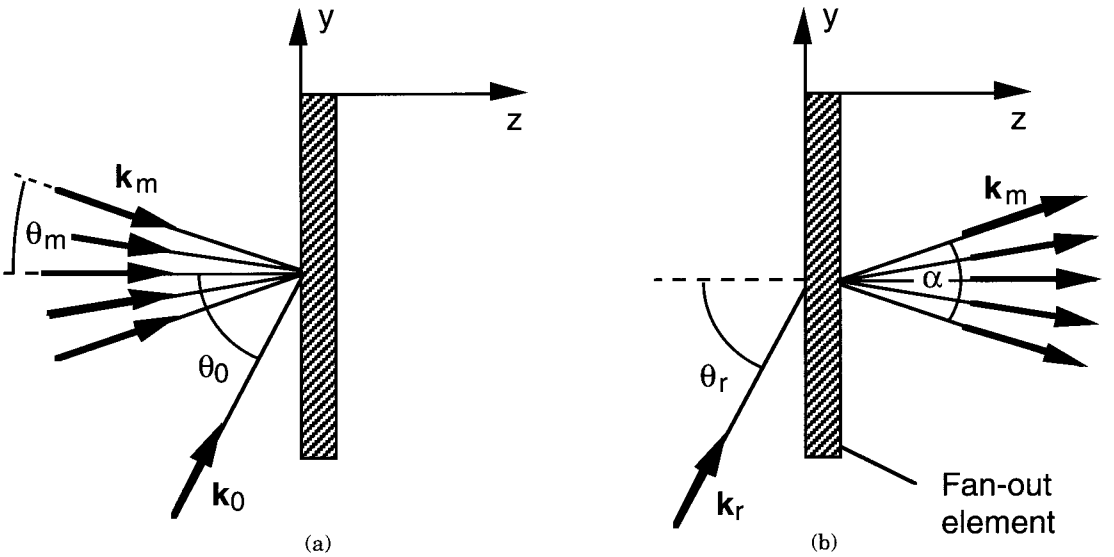

Figure 2. (a) Recording and (b) readout of fan-out elements. The angles are defined inside the recording medium, α is the full fan-out angle.

be compensated by holographic recording. The principle consists of replacing the detectors with coherent object sources, which are then recorded including the error of the optical elements in the beam path. The implementation of this approach for multifacet holograms is straightforward. However, for the recording of multiplexed fan-out elements, a key problem is the generation of "phase optimized sources," which is the main subject of this paper.

In particular, Sec. 2 describes the recording of highly efficient multiplexed fan-out gratings. For this purpose, sequential and simultaneous multiple-beam recordings will be analyzed. It is shown that the relative phases of the object beams have a strong impact on the achievable performance. Optimum recording conditions and recording material limitations are discussed. Experimental results for simultaneously and sequentially recorded volume holograms will be presented.

In Sec. 3, the concept of optimized multiple-beam recording is applied to demonstrate efficient surface-relief holograms in photoresist.

Stray light is a main limitation for the application of diffractive elements in micro-optical systems. In the case of HOEs, the main contribution to stray light comes from the undiffracted light in the reference wave. This component is difficult to separate spatially from the generated object beam for compact optical systems. In Sec. 4, we show that total internal reflection (TIR) holography offers an elegant solution to this problem. We present a simultaneous recording approach that, combined with TIR holography, enables the generation of a large number of lenslets with small focal lengths. Fabricated elements are presented in reconfigurable interconnection systems and for optical clock signal distribution on a VLSI chip.

We discuss here the recording of fan-out elements and multifacet holograms. However, the principles are also valid for the holographic recording of more general structures. The basic concepts are important to store a maximum of information in a physical recording medium and are therefore related to the recording of holographic memories.

Fan-Out Gratings Recorded as Volume Holograms

Multiple-Beam Recording. A fan-out hologram can be realized by recording the interference pattern of N object waves $E_m(\mathbf{x}) = A_m \exp(-i\mathbf{k}_m\mathbf{x} + i\phi_m)$ and an off-axis reference wave $E_0(\mathbf{x}) = A_0\exp(-i\mathbf{k}_0\mathbf{x} + i\phi_0)$. The basic configuration is shown in Fig. 2. The recording beams are plane waves characterized by their wavevectors $\mathbf{k}_i = (k_i^y, k_i^z)$, amplitudes A_i, and relative phases ϕ_i, where $i = 0$ denotes the reference wave. The result of the recording process is a multiplexed grating hologram that can be constructed by either simultaneous or sequential recording. Readout at the Bragg angle is considered. Focusing of the generated object beams on the detector array is achieved by an additional lens that is not shown.

In the case of simultaneous recording all object beams and the reference beam are recorded in one exposure. Assuming a linear response of the material, the recorded dielectric permittivity $\varepsilon(\mathbf{x})$ becomes

$$\varepsilon(\mathbf{x}) = \varepsilon_a + \delta\left|\sum_{m=1}^{N} E_m + E_0\right|^2 = \varepsilon_a' + P(\mathbf{x}) + M(\mathbf{x}), \tag{1}$$

where

$$\varepsilon_a' = \varepsilon_a + \delta(A_0^2 + NA^2), \tag{2}$$

$$P(\mathbf{x}) = 2\delta A_0 A \sum_{m=1}^{N} \cos(\mathbf{K}_{0m}\mathbf{x} - \Phi_{0m}), \tag{3}$$

$$M(\mathbf{x}) = 2\delta A^2 \sum_{n>m=1}^{N} \cos(\mathbf{K}_{mn}\mathbf{x} - \Phi_{mn}). \tag{4}$$

Besides the N desired primary gratings $P(\mathbf{x})$, resulting from the interference of the reference wave and each object wave, $N(N-1)/2$ additional intermodulation gratings $M(\mathbf{x})$ are recorded. These intermodulation gratings result from the interference between the object waves. The primary gratings $P(\mathbf{x})$ and the intermodulation gratings $M(\mathbf{x})$ are defined by their grating vectors $\mathbf{K}_{pq} = \mathbf{k}_p - \mathbf{k}_q$ and their relative positions are fixed by the phases $\Phi_{pq} = \Phi_p - \Phi_q$ $(p,q = 0, \ldots, N)$. The constant values ε_a and ε_a' are the average permittivity before and after exposure. For the recording of a uniform fan-out element, equal object beam amplitudes $A_m = A$ are applied.

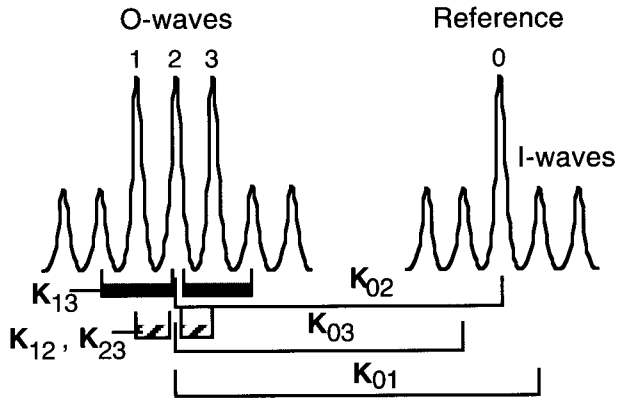

Figure 3. Spectrum of the waves included in our coupled-wave model for a fan-out of $N = 3$ object waves (O-waves), and possible interactions for object wave (O-wave) 2 through primary gratings $\mathbf{K}_{0m}$ and intermodulation gratings $\mathbf{K}_{mn}$. The same intermodulations have been considered for the other objects waves (O-waves 1 and 3).

The recording geometry is chosen such that the recorded primary gratings are optically thick and reconstruct essentially one object beam. However, since the interobject beam angle $\Delta\alpha = \alpha/(N-1)$ is small ($\Delta\alpha < 1°$), the recorded intermodulations are in general optically thin and couple energy to several diffraction orders.

To study the reconstruction properties of multiplexed holograms, a coupled wave model has been developed.[6] Figure 3 shows the spectrum of the generated waves at readout. The analysis has shown that the following interactions are important:

1. The reference wave is diffracted at the primary gratings $\mathbf{K}_{0m}$ and reconstructs the desired object waves (O-waves).
2. The reference wave is diffracted also at the thin intermodulation gratings $\mathbf{K}_{mn}$ and generates intermodulation waves (I-waves).
3. Secondary diffraction: All waves that are generated by the reference wave are diffracted again at all gratings.

The coupled wave analysis of multiple-beam recording has shown that high efficiency (>90%) can be achieved if the intermodulation gratings and the secondary diffraction can be eliminated.[6] In the following, we discuss the necessary precautions.

One possibility to reduce the intermodulation effects is to increase at recording the reference-to-object beam ratio. Then, the modulation of the primary gratings becomes dominant compared with the modulation of the intermodulation gratings. However, a high beam ratio does not eliminate secondary diffraction at primary gratings, which limits the achievable diffraction efficiency.[6] In addition, this method requires a high dynamic range for the recording material and is therefore not recommended.

In the case of *simultaneous recording*, undesired intermodulation gratings and secondary diffraction can be eliminated by optimized phases ϕ_i of the object waves.[6] The optimization procedure consists of minimizing the function $M(\mathbf{x})$ in Eq. 4 by varying $\Phi_{mn} = \Phi_m - \Phi_n$. However, this is only possible within a limited depth. Here we estimate this depth.

The intermodulation gratings vary in the z direction with K^z_{mn}. The largest component K^z_{mn} is formed by the interference between the central beam and the marginal beams of the fan-out. We obtain

$$\left(K_{mn}{}^{z}\right)_{\max} = \frac{2\pi}{\lambda} n\left(1-\cos\frac{\alpha}{2}\right) = \frac{2\pi}{\Lambda}, \tag{5}$$

where λ is the wavelength, α the full angle ($\mathbf{k}_1$,$\mathbf{k}_N$) of the fan-out, n the refractive index, and Λ the periodicity of the grating $(K^z_{mn})_{\max}$. The coupled wave simulations have shown that the intermodulations remain small within a depth of $t_1 \approx \Lambda/5$, that is,

$$t_1 = \frac{\Lambda}{5} = \frac{\lambda}{5n\left[1-\cos(\alpha/2)\right]}. \tag{6}$$

In *sequential recording* of N object beams, N subsequent exposures to each object beam and the reference are required. Equation 1 is then replaced by

$$\varepsilon(\mathbf{x}) = \varepsilon_a + \delta \sum_{m=1}^{N} \left|E_m + E_0\right|^2 = \varepsilon_a' + P(\mathbf{x}), \tag{7}$$

where now

$$\varepsilon_a' = \varepsilon_a + \delta N(A_0{}^2 + A^2). \tag{8}$$

The function $P(\mathbf{x})$ describing the primary gratings has not changed compared to simultaneous recording and depends on the phases Φ_{0m}. On the other hand, no intermodulation gratings are recorded. Nevertheless, secondary diffraction generates intermodulation waves by diffraction of the object waves at the primary gratings $\mathbf{K}_{0m}$ (see Fig. 3). For small interbeam angles $\Delta\alpha$, these interactions are only slightly off-Bragg and reduce the diffraction efficiency and the uniformity of the fan-out. Therefore, optimized phases are also important for sequential recording.

For simultaneous and sequential recording, all off-Bragg interactions (i.e., secondary diffraction) can be neglected for a phase mismatch of the coupled waves of greater than 2π after propagation through the holographic layer. Therefore, in our arrangement (Fig. 2), the off-Bragg interactions are important for a hologram thickness smaller than

$$t_2 = \frac{\lambda}{n\tan\theta_r \Delta\alpha}, \tag{9}$$

where $\Delta\alpha = \alpha/(N-1)$ is the interbeam angle between two neighboring beams, θ_r the reference beam angle at readout, λ the wavelength, and n the refractive index.

Optimum Recording Conditions. Whether simultaneous or sequential recording is preferable depends mainly on the thickness t of the holographic emulsion and the interbeam angle $\Delta\alpha$. For the discussion of optimum recording conditions, we can distinguish three domains, which are represented in Fig. 4 as a function of the hologram thickness t.

In very thick holograms ($t > t_2$, Eq. 9) all off-Bragg interactions are inefficient. High performance can be reached for sequentially recorded holograms. Since the relative phases of the object beams are not important, simultaneous recording requires a high reference-to-object beam ratio in order to eliminate intermodulations. This domain is appropriate for the recording of holographic memories.

However, in micro-optics, the high selectivity of the Bragg condition of very thick holograms is not desired. It reduces

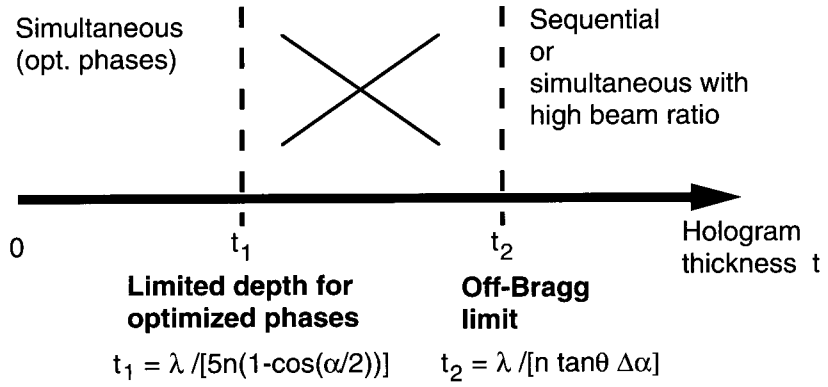

Figure 4. Domains for simultaneous and sequential recording.

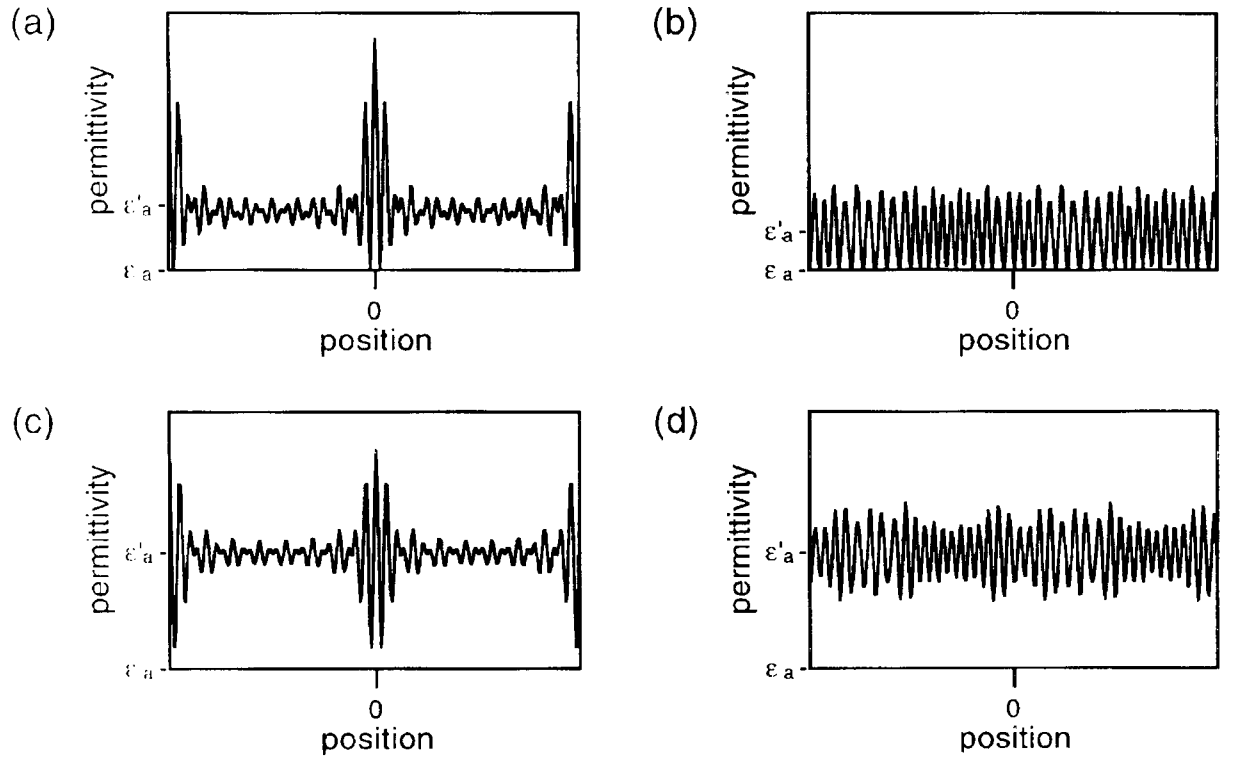

Figure 5. Permittivity modulation for recording $N = 9$ object waves with the best contrast: (a) simultaneous recording with $\phi_m = 0$, (b) simultaneous with optimum object phases, (c) sequential recording with $\phi_m = 0$, and (d) sequential with optimum object phases. The modulation $2\delta A_0 A$ of the primary gratings is identical in all cases. Note that the axes of the graphs have the same scale.

the alignment tolerances and limits also the acceptance angle for readout. A practical fan-out element should have an acceptance angle of at least several degrees. As a consequence, the emulsion thickness should be less than about 20 μm. For these holograms, the control of the relative phases of the object beams is important and the recording geometry has to be chosen in the first domain limited by the field depth t_1 (Eq. 6) of the optimized phases. In this region, simultaneous recording with optimized phases is preferential. Sequential recording with optimized phases could be applied, but requires, as will be shown in the next paragraph, a higher dynamic range.

The intermediate region, $t_1 < t < t_2$, has to be avoided, since only poor fan-out performance is achievable.

Limitations for Large Fan-Out Numbers. In this paragraph, limits are discussed for the recording of fan-out elements with a large number of object beams in a thin holographic medium (domain 1 of Fig. 4). The limits are imposed by the dynamic range of the recording medium and the limited depth of the optimized phases. Furthermore, the generation of large fan-out numbers and alignment tolerances for recording have to be considered.

Dynamic Range. For optimum hologram recording the exposure energy has to be within the dynamic range. We will show that recording with optimized phases requires a lower dynamic range.

Figure 5 shows the calculated permittivity modulation $\varepsilon(\mathbf{x})$ for (a) simultaneous recording with $\phi_m = 0$, (b) simultaneous recording with optimum object phases ϕ_m, (c) sequential recording with $\phi_m = 0$, and (d) sequential recording with optimum object phases. In all cases the contrast is optimum and the modulations $2\delta A_0 A$ of the primary gratings are identical. It is evident that more object beams can be recorded when the maximum value $\Delta\varepsilon_{max} = \varepsilon_{max} - \varepsilon_a$ is small. The lowest maximum modulation is achieved for simultaneous

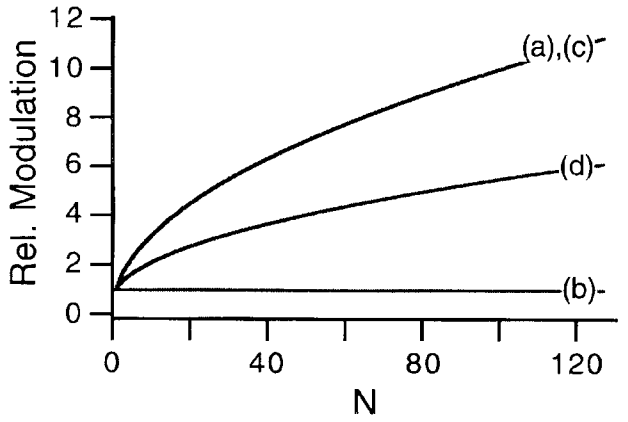

Figure 6. Relative modulation range necessary for (a) simultaneous and (c) sequential recording with worst case object phases; (b) simultaneous and (d) sequential recording with optimum object phases.

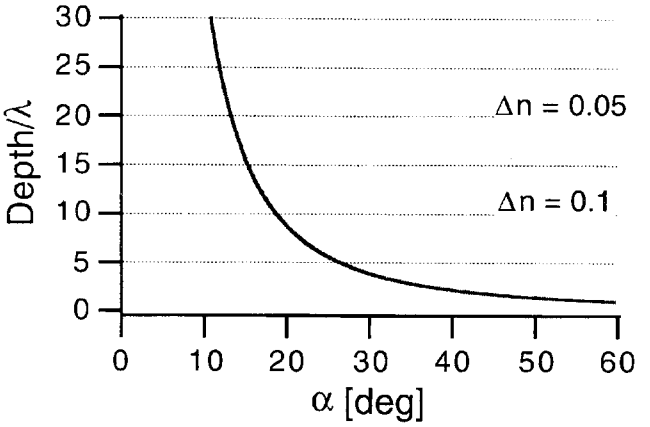

Figure 7. Depth, within which the intermodulation is minimum, versus full fan-out angle α. Maximum fan-out angle α is limited by the achievable index modulation Δn.

recording with optimized phases, case (b), where $M(\mathbf{x})$ disappears and $P(\mathbf{x})_{max} = 2\delta A_0 A\sqrt{N}$, (see Eqs. 1 – 4).

Figure 6 presents the relative modulation of the holographic emulsion as a function of the number of object beams for the different recording conditions. A relative modulation of 1 corresponds to the maximum permittivity modulation $\Delta\varepsilon_{max}$ necessary for a highly efficient hologram recorded with one object and one reference beam. For increasing N, we have to take into account that the modulation of the primary gratings necessary for optimum efficiency decreases with $\sqrt{N}$. The results show that case (b), simultaneous recording with optimized phases, is not limited by the number of object beams. It behaves as if only one object beam is present. Whereas in the worst cases, (a) and (c), a fan-out of $N = 100$ would require 10 times the modulation of a simple grating. This is difficult to achieve in thin emulsions.

Depth of the Optimum Plane. A critical point in recording a hologram with optimized object beam phases is the limited depth of the optimum plane. This depth is determined by the maximum fan-out angle α, Eq. 6. Figure 7 shows the limited depth versus the fan-out angle α for a refractive index of $n = 1.5$. The angle is given in the medium. Because a simultaneously recorded hologram with optimized object phases behaves as a single grating, high diffraction efficiency requires an optical path difference of $\Delta n\, t = \lambda$ (full length) in the holographic medium.[7] As an example, if the holographic emulsion can generate an index modulation of $\Delta n = 0.1$, then a thickness of about $t/\lambda = 1/\Delta n = 10$ is required for high diffraction efficiency. Now, it follows from Fig. 7 that a thickness of 10λ limits the maximum fan-out angle to $\alpha = 20°$.

Generation of Spot Array. The application of optimized object beam phases requires that the object beams be located on a regular grid in the focal plane. It is not necessary for the spots to form a regular pattern. The method of optimized phases works also for more general patterns with the spots located on a sampling grid. This condition generates a globally periodic object beam in the hologram plane and intermodulations can be eliminated over the whole recording plane.

If the object beam sources are not situated on a regular sampling grid, intermodulations in the hologram plane can only be eliminated over a finite distance, which limits the hologram dimensions for a successful recording.

In the following, we estimate tolerable deviations of the position of the object beam spots with respect to the regular sampling grid. Assuming diffraction-limited performance and a rectangular hologram aperture, the object beams have sinc functions as intensity distributions in the focal plane with a radius r of the first intensity zero given by $r = \lambda f/D$, where f is the focal length and D the hologram diameter. A deviation Δ of one regular spot position introduces in the hologram plane a sinusoidal intensity variation. To achieve good recording conditions, the period of this intensity variation has to be larger than the hologram diameter, which requires a deviation Δ of less than

$$\Delta < \frac{\lambda f}{D}. \tag{10}$$

Equation 10 also determines the alignment tolerances of the spot array for successful recording with optimized phases. It follows that for fast systems, submicrometer precision has to be achieved, which requires master elements fabricated by electron-beam writing for the generation of the N optimized object beams.[1]

In principle, computer-generated holograms (CGHs) or any highly-efficient on-axis fan-out element can be used to generate the phase-optimized object beams. Other possibilities are based on the Talbot effect.[8] An efficient technique that is to generate very large arrays of optimized beams is to illuminate a pinhole array, followed by an appropriate phase plate.

Experimental Results. For the experiments, we realized an array of object beams with optimized phases by means of a CGH.[9] The CGH is a binary amplitude grating with a carrier frequency of 125 lines/mm, which has been fabricated by electron-beam lithography. The phase distribution of the CGH has been calculated according to Ref. 10. The CGH is then imaged onto the hologram plane through a standard 4f lens system. The desired N object beams with optimized phases are contained in the first diffraction order of the CGH, which is spatially filtered in the Fourier plane of the 4f system.

The $N = 9$ object beams have been recorded in a dichromated gelatin layer of thickness of 15 μm at the wavelength of $\lambda = 488$ nm. We have chosen a reference beam angle of $\theta_0 = 30°$ and an interbeam angle of $\Delta\alpha = 0.057°$, which yields a spot spacing of 100 μm in the back focal plane of lens with focal length of 100 mm.

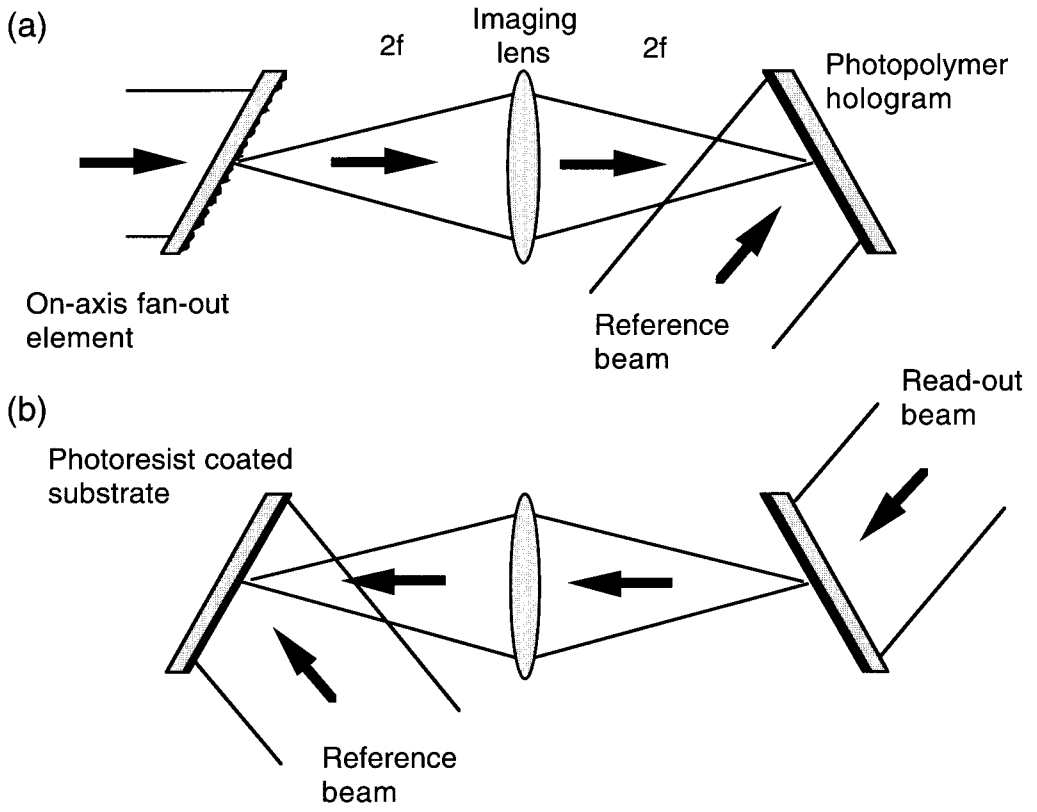

Figure 8. Self-aligned two-step recording process for off-axis fan-out gratings in photoresist. (a) Recording geometry of the intermediate volume hologram in photopolymer and (b) recording geometry of the final photoresist hologram.

In the case of simultaneous recording, the uniformity error was found to be ±5% and the overall efficiency was 84%. This corresponds to a diffraction efficiency of 94% if antireflection coatings are used.

In the case of sequential recording, we have used the same recording setup, but only two beams at a time, the reference and one of the object beams. The overall efficiency was measured at 74% and the uniformity error was ±11%.

The experimental results for sequential recording are inferior to those obtained by simultaneous recording. We assume, that the phase relationship during the nine recording steps could not be controlled sufficiently well. Higher efficiency (>90%) can be expected from an improved recording system with active phase control.

Surface-Relief Holograms

Holographically recorded elements can also be realized as surface-relief profile in photoresist.[11] The resulting binary phase elements become highly efficient for symmetric deflection if the grating periods are of the order of the wavelength. This technique is limited to simple grating-like patterns, which have high contrast. Using optimized phases, this condition can also be achieved for N object beams. Surface-relief holograms have the advantage of high index modulation (Δn = 0.5). For visible and near-infrared wavelengths, the thickness is of the order of a micron. As a consequence, they are not sensitive to angular variation of the readout beam and they can generate large fan-out angles (see Fig. 7).

Experimental results have been achieved for the recording of a 9 × 9 off-axis fan-out hologram in photoresist.[11] For the recording, a different setup has been applied. To achieve deep binary surface-relief grating structures, symmetric incidence of the reference wave and the object beam is required, which produces interference fringes perpendicular to the resist surface. As a consequence, the optimized plane of low intermodulations is tilted with respect to the propagation direction of the object beam. The accurate imaging of the optimized object wavefront and the alignment of the imaging system become difficult. We have circumvented these problems by using a two-step recording approach for the copying. The two-step recording process is schematically represented in Fig. 8.

In our experiments, the optimized fan-out phase function has been generated from an on-axis continuous-relief fan-out grating in photoresist fabricated by laser bean writing.[12] In the first recording step, an intermediate volume hologram of the object beam is recorded. This intermediate copy needs not to be recorded for high diffraction efficiency. This hologram is recorded in general with a high reference-to-object beam ratio. We have used photopolymer from Du Pont[13,14] as the holographic recording medium for the intermediate copy. The photopolymer has the advantage that it is self-developing during the exposure. The holographic plate can therefore be kept in place during the whole process, and it remains automatically aligned. At readout, the photopolymer hologram is illuminated with the conjugate reference wave. This illumination generates the conjugate object beam, which passes inversely through the same imaging system and compensates on its way for all of the acquired aberrations. The photoresist hologram can therefore be recorded in the predefined position of the original master element.

The realized elements have a carrier grating period of 577 nm, which is locally modulated by the fan-out function

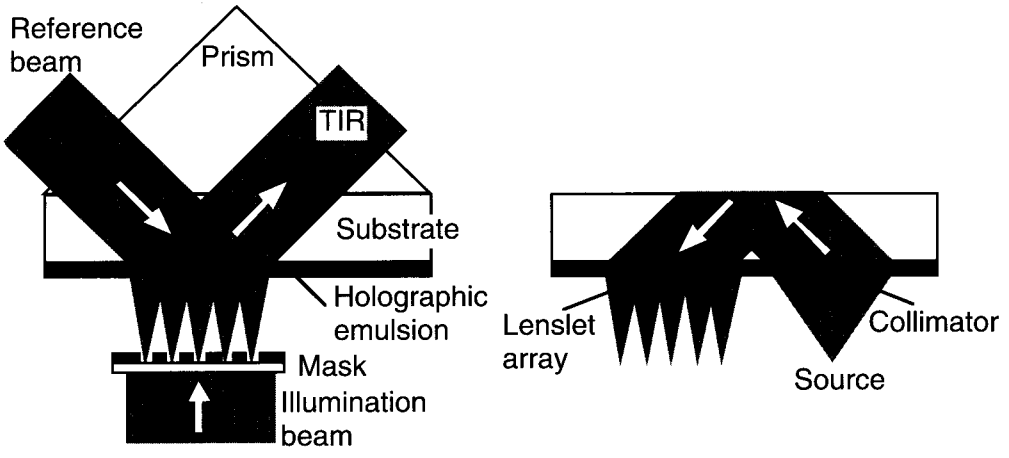

Figure 9. (a) Recording and (b) readout geometry for holographic lenslet arrays fabricated by TIR holography.

of the 400 μm period in both axes. A modulation depth in photoresist of 600 nm has been achieved, which produces at readout with a wavelength of 633 nm a diffraction efficiency of 70% and uniformity error of 13% over the whole 9 × 9 array. Higher efficiencies over 90% are feasible for deeper grating structures and can be achieved by improved photoresist processing or by plasma etching of the resist relief in the substrate material.[1,2]

TIR Holography for the Fabrication of Micro-Optical Systems

Principle of TIR Holography. An interesting concept for realizing a compact micro-optical system is TIR holography.[15] The basic principle is shown in Fig. 9(a) in the example of a holographic lenslet array. Arrays of spherical waves can be generated simultaneously by illuminating a pinhole array on a mask with a laser beam. Such masks can be fabricated by electron-beam lithography, which ensures high position accuracy of the focal points. The pinhole array mask is recorded holographically by passing a collimated beam through the mask, which is placed in proximity (typically 50 – 500 μm) to the photosensitive layer in order to prevent overlap of neighboring lenslets. The transmitted wave interferes with the reference wave, which is fed through a prism and totally reflected at the film–air interface. For the reconstruction without prism, the readout beam can be coupled into the hologram substrate by another holographic grating [Fig. 9(b)], which acts at the same time as a collimator. This coupling element can be fabricated in the same photosensitive layer as the lenslet array. The collimator and lenslet array together form a compact system. Because of its symmetry, this system is quite insensitive to wavelength changes. Furthermore, unwanted stray light is captured within the substrate. A problem of the TIR method is that three beams (reference beam, TIR beam, object beam) are involved in the hologram recording, which limits in general the diffraction efficiency at readout. The diffraction behavior of TIR holograms has been studied in Refs. 16 and 17 and conditions for high diffraction efficiency are derived therein.

Near-field TIR holography plays an important role in planar optics. The planar integration of free-space optical components is a very attractive concept for optical interconnections.[18] Constraining an optical beam within a block of glass using total internal reflection offers a number of advantages for optical system construction: modularity, compactness, mechanical stability, lack of turbulence, and reduced number of interfaces. The optical devices are placed on the surface of a glass block and index-matched to the block. This concept allows all optical devices to be aligned with submicron precision in the same microlithographic process.

The most attractive sources for optical interconnections are laser diodes emitting at near-infrared wavelengths, whereas common recording materials are only sensitive to visible or ultraviolet light. The resulting wavelength shift between recording and readout leads to aberrations and also to a reduction in diffraction efficiency. Many different schemes have been presented in the literature in order to compensate for aberrations and efficiency by using one or two CGHs for recording. However, these approaches are not suitable for production, since all the elements have to be aligned precisely with respect to each other.

In micro-optics, small-diameter lenslets are of interest. Because for a fixed f number, aberrations increase with the lens diameter, good optical performance for microlenses can be achieved without aberration-corrected wavefronts. Low aberrations and high diffraction efficiency can be achieved by applying a two-step recording process.[19] In the first step, spherical wavefronts emanating from the pinhole mask are recorded in the holographic film at the final reconstruction angle. Then, in the second step, the Bragg angle is adjusted for high diffraction efficiency. For volume holograms, this is achieved by contact printing, whereas for surface-relief holograms the Bragg angle can be adjusted by ion-beam etching with oblique incidence.[20]

To test the performance of near-field TIR holography, we have fabricated a regular 100 × 100 lenslet array and also a nonregular lenslet array for clock distribution to a specially designed integrated circuit.

High-Density Multifacet Holograms. A chromium mask with 100 × 100 pinholes equally distributed on a surface of 1 cm^2 was realized by electron-beam lithography. The pinholes have a size of 10 × 10 μm^2 and a spacing of 100 μm. To avoid undesirable overlapping of the object waves, we placed the mask about 400 μm from the holographic emulsion and recorded it with the described near-field TIR method.

At readout, the holographic lenslet array produces diffraction-limited spots with a focal length of 390 μm and a

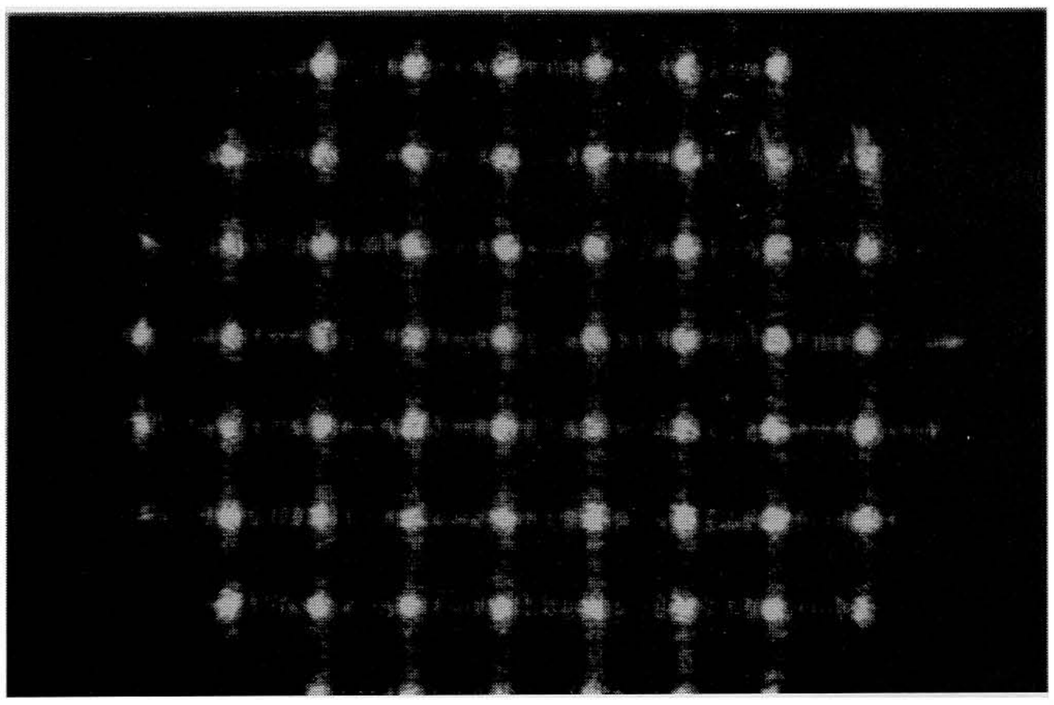

Figure 10. Foci generated by the 100×100 lenslet array. The spot size is 10 μm and the separation between two spots is 100 μm.

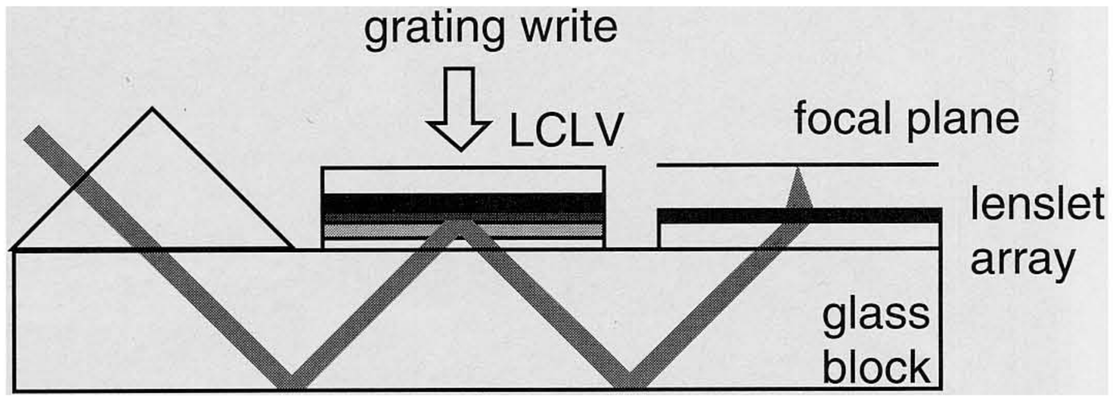

Figure 11. Reconfigurable interconnections in planar optics. The optical system is mounted on a glass substrate. The collimated light beam is coupled into the substrate with a prism. The substrate mode beam is reflected by the liquid crystal light valve (LCLV) and reaches the holographic lenslet array, which focuses the light in the output plane. Depending on the period and the orientation of the grating written on the LCLV, different locations of the lenslet array can be attained.

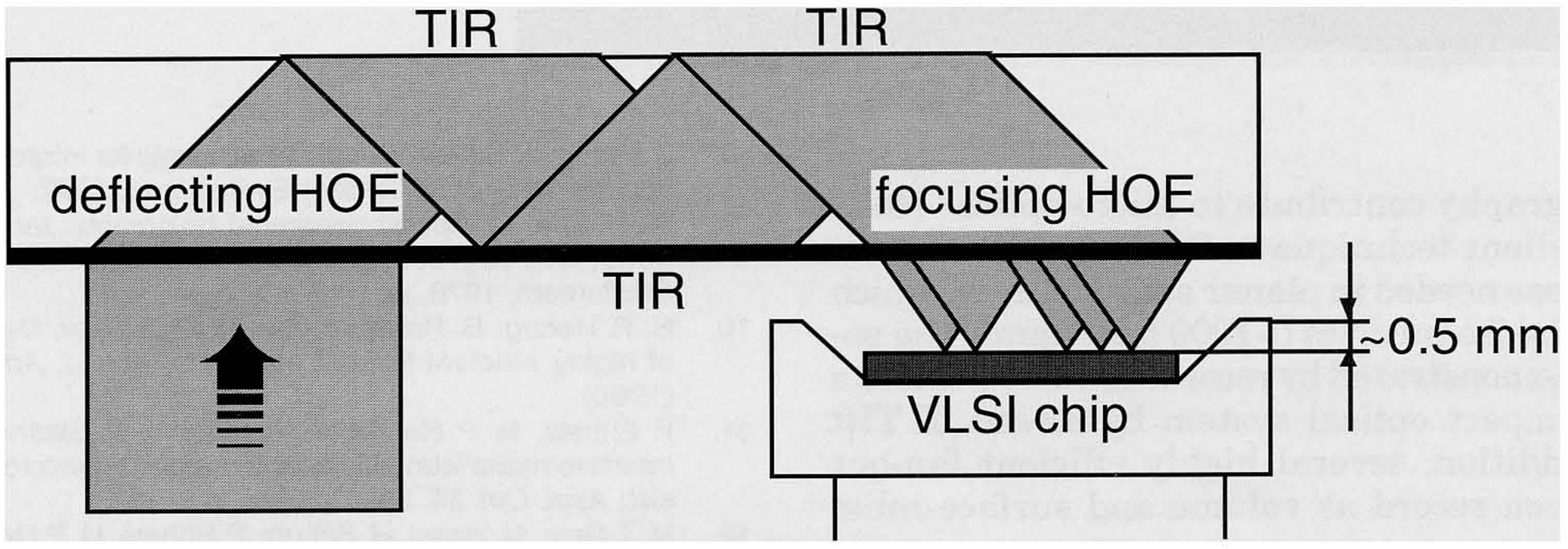

Figure 12. Geometrical configuration at readout. The readout laser beam ($\lambda = 488$ nm) is coupled in the glass substrate with a deflecting HOE. After four successive total internal reflections (TIRs), the beam reaches the focusing HOE. The hologram is placed 1 mm above the VLSI circuit which is covered with a glass window.

size of about 10 μm. Figure 10 shows part of the generated spot pattern.

An application for this lenslet array has been described and realized by Collings et al.[21] The lenslet array has been used together with a liquid crystal light valve (LCLV) to form a reconfigurable interconnection system. The optical system is mounted on a glass substrate (planar optic) as shown in Fig. 11. The collimated light beam is coupled into the substrate with a prism. The substrate mode beam is reflected by the LCLV (a ferroelectric liquid crystal/amorphous silicon photoconductor sandwich) and reaches the holographic lenslet array, which focuses the light in the output plane. When a 10 lines/mm grating is written on the LCLV, then two diffracted spots appear in the focal plane of the lenslet array. These are the +1 and −1 diffracted orders of the substrate mode beam. The diffracted spots are displaced by about 10 lenslets from the central spot. Depending on the period and the orientation of the grating written on the LCLV, different locations of the lenslet array can be attained. Note, that in this configuration the LCLV must show good off-axis performance and the off-axis lenslet array must have a "broad" angle acceptance ($45° \pm 3°$ in our case).

Such programmable beam deflectors are attractive for $N \times N$ circuit switch applications. With this configuration, the link insertion loss is independent of the parallelism of the interconnection network. This is important when compared with other switching options such as the matrix-vector-multiplier optical crossbar, where the losses scale at least linearly with the number of links.

Clock Distribution HOE for a VLSI Circuit. We have also applied the TIR method to the fabrication of a nonregular lenslet array for demonstrating clock distribution to a real VLSI circuit.[19] For that purpose, a special test chip has been realized at the CSEM (Centre Suisse d'Electronique et de Microtechnique) in Neuchâtel using CMOS technology (CMN20A of VTI). Its outer dimensions are 3×3 mm^2. Several arrays of photodetectors with different sizes from 3×3 to 100×100 μm^2 are integrated on the chip. The chip contains also transimpedance amplifiers ($R = 1$ MΩ) and output buffers to interface the photodiodes with the external electronics.

For the TIR hologram recording, a special pinhole chromium mask was fabricated by electron-beam lithography. Each pinhole corresponds to a detector on the integrated circuit and acts as a source when illuminated with a laser beam. The HOE has been recorded in a Du Pont photopolymer using an argon laser at $\lambda = 488$ nm.

The readout configuration is shown in Fig. 12. The readout laser beam ($\lambda = 488$ nm) is coupled in the glass substrate with a deflecting HOE. After four successive TIRs, the beam reaches the focusing HOE. The hologram is placed 1 mm above the VLSI circuit, which is covered with a glass window.

Figure 13 shows the reconstructed spot pattern projected onto the VLSI circuit. One can see that all patterns are properly reconstructed. It has been demonstrated,[22] that the near-field TIR method is capable of reproducing structures down to 0.4 μm at $\lambda = 488$ nm.

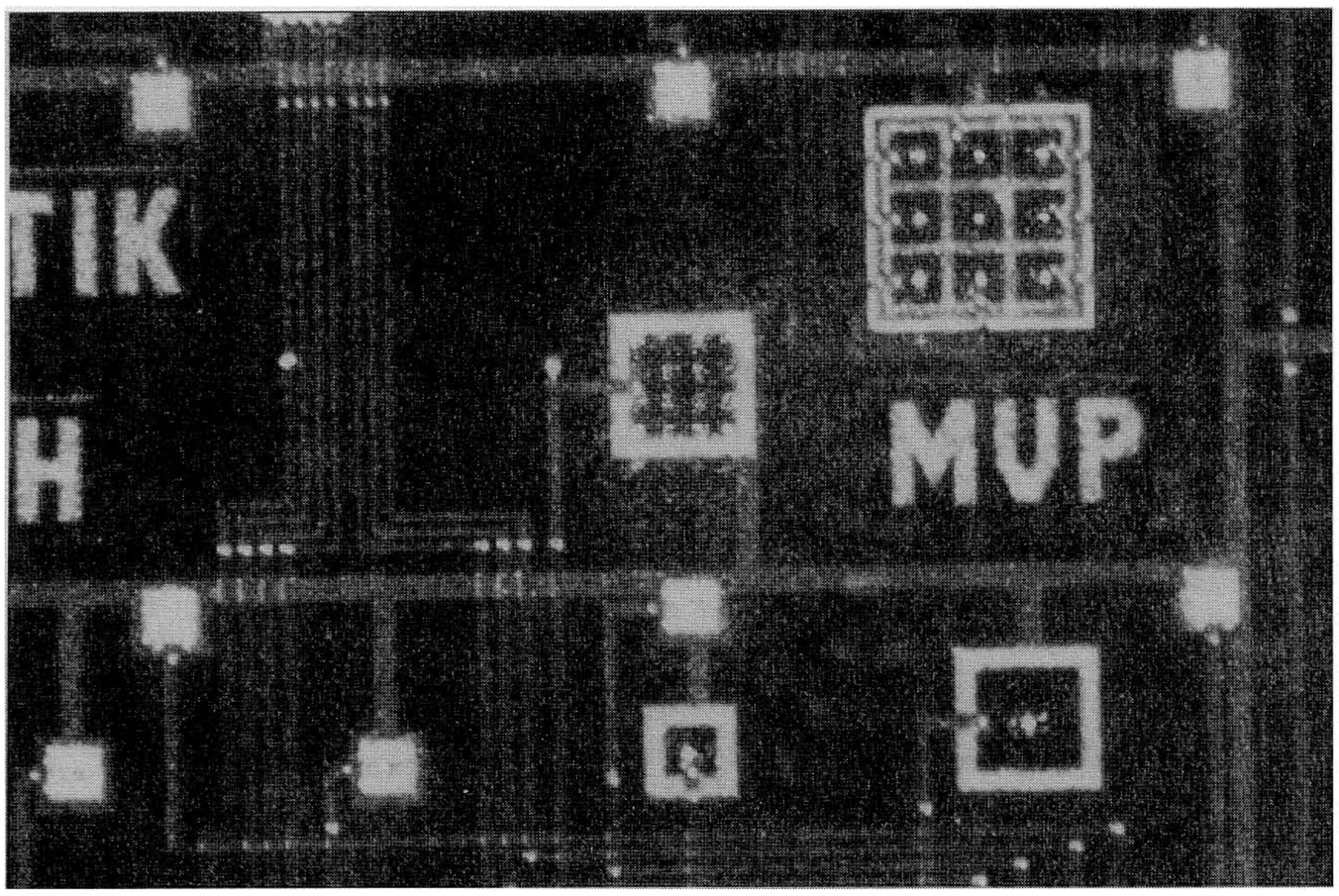

Figure 13. Reconstructed spot pattern projected onto the VLSI circuit, as shown schematically in Fig. 12. One can see that all patterns are properly reconstructed. The spacing between the spots of the 3 × 3 array in the upper right corner is 60 μm.

Conclusions

What can holography contribute to micro-optics? Holography is an excellent technique to fabricate off-axis elements, such as those needed in planar architecture's, which require high spatial frequencies (>1000 lines/mm). The potential has been demonstrated by recording 10,000 lenslets on 1 cm^2 in a compact optical system by means of TIR holography. In addition, several highly efficient fan-out elements have been record as volume and surface-relief holograms.

An emphasis was given to the optimum recording of complex object beams in order to get highly efficient holograms. For this purpose, sequential and simultaneous multiple-beam recording has been analyzed. Optimum recording conditions and recording material limitations were discussed.

References

1. H. P. Herzig, M. T. Gale, H. W. Lehmann, and R. Morf, Diffractive components: computer-generated elements, in *Perspectives for Parallel Optical Interconnects*, Ph. Lalanne et P. Chavel, Eds., Springer-Verlag, Berlin, 1993, pp. 71–107.
2. H. P. Herzig, Ed., *Micro-Optics: Elements, Systems, and Applications*, Taylor & Francis, London, 1997.
3. M. J. Verheijen, E-beam lithography for digital holograms, *J. Mod. Opt.* **40**, 711 (1993).
4. S. J. Walker, J. Jahns, L. Li, W. M. Mansfield, P. Mulgrew, D. M. Tennant, C. W. Roberts, L.C. West, and N.K. Ailawadi, Design and fabrication of high-efficiency beam splitters and beam deflectors for integrated planar micro-optic systems, *Appl. Opt.* **32**, 2494 (1993).
5. J. Saarinen, E. Noponen, J. Turunen, T. Suhara, and H. Nishihara, Asymmetric beam deflection by doubly grooved binary gratings, *Appl. Opt.* **34**, 2401 (1995).
6. H. P. Herzig, P. Ehbets, D. Prongué, and R. Dändliker, Fan-out elements recorded as volume holograms: optimized recording conditions, *Appl. Opt.* **31**, 5716 (1992).
7. H. Kogelnik, Coupled wave theory for thick hologram gratings, *Bell Syst. Tech. J.* **48**, 2909 (1969).
8. D. Prongué, Diffractive optical elements for interconnections, *PhD Thesis* University of Neuchâtel, Switzerland, 1992.
9. W. H. Lee, Computer-generated holograms: techniques and applications, in *Progress in Optics XVI*, E. Wolf, Ed. North-Holland, Amsterdam, 1978, pp. 119–232.
10. H. P. Herzig, D. Prongué, and R. Dändliker, Design and fabrication of highly efficient fan-out elements, *Jpn. J. Appl. Phys.* **29**, L 1307 (1990).
11. P. Ehbets, H. P. Herzig, P. Nussbaum, P. Blattner, and R. Dändliker, Interferometric fabrication of modulated submicron gratings in photoresist, *Appl. Opt.* **34**, 2540 (1995).
12. M. T. Gale, M. Rossi, H. Schutz, P. Ehbets, H. P. Herzig, and D. Prongué, Continuous-relief diffractive optical elements for two-dimensional array generation, *Appl. Opt.* **32**, 2526 (1993).
13. A. M. Weber, W. K. Smother, T. J. Trout, and D. J. Mickish, Holographic recording in Du Pont's new photopolymer materials, in *Practical Holography IV*, *Proc. SPIE* **1212**, 30 (1990).
14. W. J. Gamboni, W. A. Gerstadt, S. R. Mackara, and A. M. Weber, Holographic transmission elements usingimproved photopolymer films, in *Computer and Optical Generated Holographic Optics (Fourth in a Series)*, *SPIE Proc.* **1555**, 256 (1992).
15. K. Stetson, Holography with total internally reflected light, *Appl. Phys. Lett.* **11**, 225 (1967).
16. P. Ehbets, H. P. Herzig, and R. Dändliker, TIR holography analyzed by coupled wave theory, *Opt. Commun.* **89**, 5 (1992).
17. P. Ehbets, H. P. Herzig, M. Kuittinen, F. S. M. Clube, and Y. Darbellay, High-carrier-frequency fan-out gratings fabricated by total internal reflection holographic lithography, *Opt. Eng.* **34**, 2377 (1995).
18. J. Jahns and A. Huang, Planar integration of free-space optical components, *Appl. Opt.* **28**, 1602 (1989).
19. D. Prongué and H. P. Herzig, Total internal reflection (TIR) holography for optical interconnects, *Opt. Eng.* **33**, 636 (1994).
20. J. M. Lerner and J. P. Laude, New vistas for diffraction gratings, *Laser Focus/Electro-Optics*, May 1983.
21. N. Collings, D Prongué, and H. P. Herzig, Two-dimensional reconfigurable interconnect in a planar optics configuration, in *OSA Proceedings on Photonic Switching*, H. S. Hinton and J. W. Goodman, Eds., Vol. 8, pp. 81–84, Optical Society of America, Washington, DC (1991).
22. R. Dändliker and J. Brook, Holographic photolithography for submicron VLSI structures, in *Holographic Systems, Components and Applications*, Conference Publication **311**, Institution of Electrical Engineers, London, 1989, pp. 127–132.